RSC Publishing Faraday Discussions

Catalyst Design Insights from Modelling a Titanium-Catalyzed Multicomponent Reaction

Journal:	*Faraday Discussions*
Manuscript ID	FD-ART-04-2019-000033.R1
Article Type:	Paper
Date Submitted by the Author:	01-May-2019
Complete List of Authors:	Aldrich, Kelly; Michigan State University, Chemistry Kansal, Dhwani; Michigan State University Odom, Aaron; Michigan State University,

Faraday Discussions

ARTICLE

Catalyst Design Insights from Modelling a Titanium-Catalyzed Multicomponent Reaction

Received 00th January 20xx,
Accepted 00th January 20xx

DOI: 10.1039/x0xx00000x

www.rsc.org/

Kelly E. Aldrich, Dhwani Kansal, and Aaron L. Odom*

High oxidation state transition metal catalysis touches our daily lives through bulk chemical production, e.g., olefin polymerization, and through specialty chemical reactions common in organic synthesis, e.g., Sharpless asymmetric epoxidation and olefin dihydroxylation. Our group has been expanding the reaction chemistry of titanium(IV) to produce a host of nitrogen-based heterocycles via multicomponent coupling reactions. One such multicomponent coupling reaction discovered in our laboratory is iminoamination, involving an amine, alkyne, and isonitrile. However, experimental modeling of high oxidation state reactions lags far behind low oxidation state systems where a great deal is known about ligands, their donor properties, and how their structures affect catalysis. As a result, we have developed an experimental method for determining the donor abilities of anionic ligands on high oxidation state systems, which is based on the chromium(VI) nitride system $NCr(N^iPr_2)_2X$, where X = the ligand being interrogated. The parameters obtained are simply called Ligand Donor Parameters (LDP). In this contribution, a detailed optimization of the $Ti(NMe_2)_2$(dpm)-catalyzed iminoamination reaction was carried out, where dpm = 5,5-dimethyldipyrrolylmethane. In the course of these studies, dimeric $\{Ti(\mu\text{-N-tolyl})(dpm)\}_2$ was isolated, which is proposed as the resting state of the catalyst. To destabilize this resting state, a more electron-rich bis(aryloxide) catalyst system was investigated. The more electron-rich system is somewhat more active for iminoamination uner some conditions; however, the catalyst is prone to disproportionation. A study of heteroleptic titanium complexes revealed that the disproportionation equilibrium constant can be effectively modeled as a function of the square of the difference in LDP between the ligands, $(\Delta LDP)^2$. Using this methodology one can estimate the stability of titanium complexes toward disproportionation.

Introduction and Background

High oxidation state transition metals are of great importance to many different bond-making processes. An obvious application of metals in their highest oxidation state is in the oxidation of organic substrates, for which titanium(IV)-catalyzed Sharpless asymmetric epoxidation of allylic alcohols and osmium(VIII)-catalyzed olefin dihydroxylation are excellent examples.[1-5] Titanium in particular is used for many different catalytic reactions[6] like olefin polymerizations,[7-12] allylation of aldehydes with dienes in the presence of reductant,[13] hydroaminoalkylation,[14-31] and multicomponent couplings.[32-49]

Our group has focused on the development of new multicomponent coupling reactions using titanium catalysts, and their applications to heterocyclic synthesis.[48] For example, we discovered a new titanium-catalyzed process for the production of tautomers of 1,3-diimines by formal addition of an iminyl and amine group to an alkyne, iminoamination.[35] The reaction involves the coupling of a primary amine, alkyne, and isonitrile and is shown in generic form in Scheme 1, with some examples of heterocycles that may be prepared from the multicomponent product in one-pot procedures.[48]

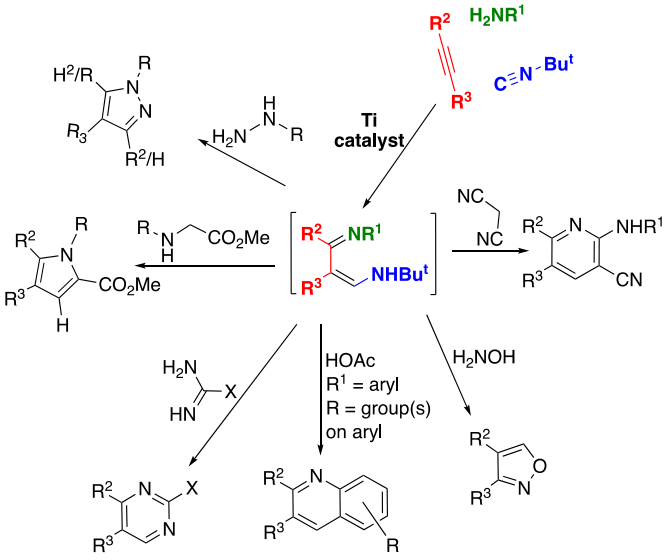

Scheme 1. Titanium-catalyzed coupling of a primary amine, alkyne, and isonitrile (iminoamination of an alkyne) to generate tautomers of 1,3-diimines, and examples of heterocycles that can be accessed in one-pot reactions from the multicomponent coupling product.

Michigan State University, Department of Chemistry, 578 S. Shaw Ln. East Lansing, MI, 48824, USA.

Electronic Supplementary Information (ESI) available: Additional experimental details for kinetics and kinetic modelling. Detailed experimental procedures for new compounds and characterization data. Data from single-crystal X-ray diffraction studies has been submitted to the CCDC in cif format and assigned index numbers: 1905879-87, 1907833-6. See DOI: 10.1039/x0xx00000x

The syntheses of the heterocycles briefly shown in Scheme 1 are only as good as the catalysis used to prepare the iminoamination product. Consequently, all of these one-pot syntheses to generate useful, pharmacologically-important heterocycles can be improved by better catalysis.

Understanding the mechanism of catalysis is exceedingly useful with regards to the design of new catalytic reactions. However, once the catalytic reaction is working and one is involved in catalyst design, mechanistic information is, in some ways, one step removed from what the experimentalist would like to know. A complete knowledge of the mechanistic pathway will tell you what transition state you want to stabilize, what ground state you want to destabilize, etc. to increase the rate of catalysis, for example, but it doesn't in and of itself tell you how best to modify the catalyst to accomplish those goals. Complementary to the mechanistic information is what ancillary ligand alterations will specifically lead to improved catalysis. Systematic investigations of ligand effects help to answer the question, what experiment do I try next?

Computational methods can facilitate mechanistic understanding and can give the type of information eluded to above by calculating pathways with a variety of different ligands on the metal. However, experiments incorporate all the untidy realities of the actual reaction that are difficult to include computationally, such as solvent effects, unknown but consistently present impurities in the starting materials or catalyst, etc. How can we efficiently get the desired information about ligand effects from experiments?

Methods for examination of ligand donation and sterics for common low valent ligands, e.g., phosphines, have been in the literature for about 5 decades, with perhaps the best-known system using the Tolman Electronic Parameter, which was based on CO stretching frequencies in $Ni(CO)_3L$, and Tolman Cone Angle, which was based on physical space-filling models of the phosphines.[50] However, there was no general method for parameterization of donor abilities of ligands commonly used for high oxidation state catalysis.

In 2012,[51] we published our first paper on using the chromium-based system $NCr(N^iPr_2)_2X$, where X = ligand being interrogated, for parameterizing ligand donor abilities for high oxidation state systems. The system works by measuring the rate constant for diisopropylamide rotation using Spin Saturation Transfer in the ^1H NMR. The rate is converted to an estimated free energy barrier using the Eyring Equation. We assume that the entropy of activation is constant, which seems to hold well for neutral complexes,[52] and using the Gibbs equation we can calculate a temperature-independent enthalpy of activation. This estimated enthalpy of activation for amide rotation is what we have dubbed the Ligand Donor Parameter (LDP). Like the Tolman Electronic Parameter, LDP gives a single parameter for total donation, $\sigma + \pi$, and as LDP increases the total donation from X is decreasing. Some examples are shown in Figure 1. Note, for LDP to be a reasonable parameter for a system's ligand effects, the metal center should have empty π-acceptor orbitals, as most high oxidation state, early transition metals do.

LDP has been found to correlate with several types of data from a variety of different high oxidation state systems. The parameters for *para*-substituted phenolates correlate with Hammett parameters. The ^{13}C NMR chemical shifts for the alkylidene-like carbon in a tungsten(VI) system with various X ligands correlates with the LDP for X. The calculated overlap of the halides and E^{t}Bu ligands with Cr, where E = O, S, Se, and Te, correlate with LDP. Ion pairing and solvation effects have been studied using LDP as a probe. In addition, the rate constant for titanium-catalyzed hydroamination of alkynes can be modelled in detail using LDP and a steric parameter.[51-56]

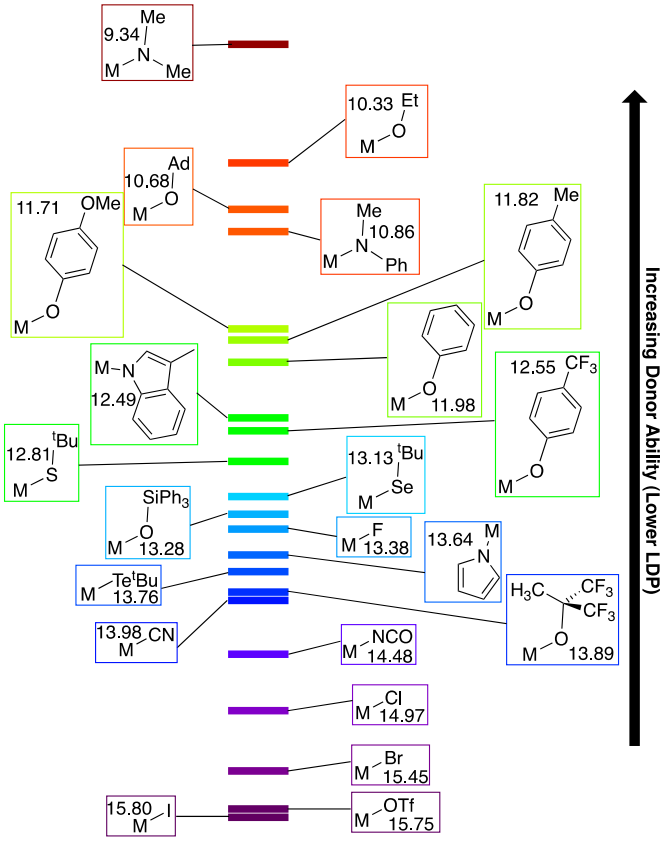

Figure 1. Examples of Ligand Donor Parameters for various ligand types. Parameters are in kcal/mol and have accuracies of ±0.1. Lower LDP values indicate greater donor abilities. Values were calculated assuming $\Delta S^{\ddagger} = -9$ e.u.

With these demonstrated correlations between the donor properties of ancillary ligands in high oxidation state metal systems and LDP, we sought to extend LDP to the optimization process for titanium-catalyzed iminoamination (Scheme 1) and related processes. This strategy combines mechanistic insights with the experimentally determined effects of ancillary ligands gained from the LDP system.

In this study, the active species in iminoamination was hypothesized to be a monomeric titanium imide with a low coordination number, which suggested that a more electron-rich ancillary ligand set may discourage dimerization and coordination of donor species to provide a more active catalyst. A more electron-rich precatalyst was found to increase the amount of monomeric imide, the proposed active species; however, a new catalyst degradation pathway was observed,

catalyst disproportionation. LDP was used to rationally design catalysts, study a catalyst degradation pathway competing with iminoamination, and even model the catalyst degradation.

Table 1. Conditions explored for iminoamination using $Ti(NMe_2)_2(dpm)$ as catalyst.[a]

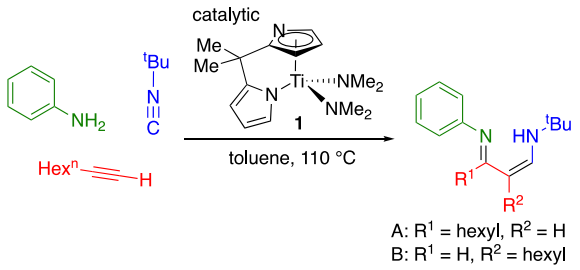

	$[1]_i$ (mol%)	$[H_2NPh]_i$	$[^tBuNC]_i$	$[1\text{-oct}]_i$	GC Yield (%)	A:B	HA (%)[b]
1	0.02 (10)	0.20	0.20	0.20	63	1.0:1	4
2	0.04 (20)	0.20	0.20	0.20	57	1.2:1	8
3	0.01 (5)	0.20	0.20	0.20	63	0.9:1	3
4	0.01 (5)	0.20	0.20	0.40	65	0.9:1	3
5	0.01 (5)	0.20	0.20	1.00	63	1.0:1	2
6[c]	0.01 (5)	0.20	0.40	0.20	61	0.9:1	3
7	0.01 (5)	0.40	0.20	0.20	77	0.9:1	4
8	0.01 (5)	1.00	0.20	0.20	80	0.8:1	4
9[d]	0.01 (5)	0.20	0.20	0.20	0[e]	—	0

[a]All concentrations in mol/L. The yield given is for both regioisomers and was determined by GCFID relative to dodecane internal standard, which was calibrated with an isolated sample of the iminoamination product. [b]The hydroamination (HA) product was quantified similarly to iminoamination product. [c]This sample, with additional ^tBuNC relative to the other runs shows a more significant amount of a 4-compound coupling product, a 2,3-diaminopyrrole.[34] [d]This run included 0.02 M iminoamination product added to the reaction mixture with the isonitrile and alkyne prior to heating samples. [e]No product, over that added at the beginning of the reaction, was observed.

The Iminoamination Reaction

As mentioned above, mechanistic information and the effects of the ligands on the reaction are complimentary information we can use to understand and improve catalysis. In order to better understand the mechanism of the iminoamination reaction, we carried out kinetic trials, varying conditions for a single substrate or parameter on each run. More details on these reactions can be found in the Supplementary Information. The best conditions investigated (Table 1) used an excess of aniline (5 equiv), 1 equiv each of alkyne and isonitrile, along with 5 mol % $Ti(NMe_2)_2(dpm)$ (**1**). These conditions gave 80% yield of the iminoamination product with minimal side reactions. Using these conditions, the hydroamination byproduct was present in 4% yield, for example. The reaction occurs with poor regioselectivity, but that is inconsequential for the kinetic studies (vide infra), which simply relied on total product concentration.

The catalyst investigated was one we most commonly employ, pyrrole-based $Ti(dpm)(NMe_2)_2$ (**1**), the structure of which is shown in the header of Table 1. The relatively low donor ability of pyrrole-based dpm is contrasted with the strongly donating and strongly basic dimethylamides, which are present in the precatalyst to act as protolytic leaving groups to form the active imide catalyst. This difference in LDP values for pyrrolide and dimethylamide turns out to be advantageous to precatalyst stability (vide infra).

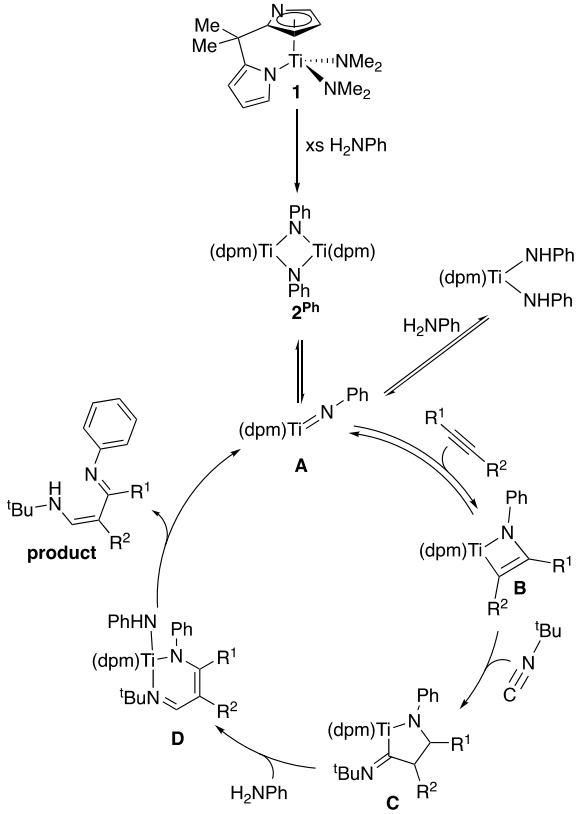

Scheme 2. (*top*) The best conditions investigated and (*bottom*) the proposed mechanism for the iminoamination reaction. R^1 and R^2 = H or *n*-hexyl in the reactions most studied in this work.

Scheme 2 shows the proposed pathway for the iminoamination reaction. While we have not been able to isolate any of the intermediates along the proposed catalytic pathway using the dpm ancillary ligand, Mountford, Gade, and coworkers have reported isolating species similar to **A**, **B**, and **C** with different ancillary ligands on the metal. The bis(amide) and imide **A** are known in other related species as well. Additionally, the nacnac-like complex **D** has been observed in very similar reactions.[57, 58]

One interesting finding during these studies was that the major byproduct, hydroamination of the alkyne (HA), was formed between reagent mixing and the reaction reaching reaction temperature. Once the reaction reached the

temperature for iminoamination, very little if any further HA product was formed.

We have directly observed the imide dimer, and this dimer is possibly the resting state of the reaction. We isolated and structurally characterized the dimer with *p*-tolylamine, {Ti(N-*p*-tolyl)(dpm)}$_2$ (**2^{tol}**), which can be prepared by simple addition of H_2N-*p*-tol to **1** and isolated in 55% yield (Figure 2). In the solid state, **2^{tol}** exists as a dimeric species and resides on a crystallographic inversion center. Each dpm ligand has one η^5-pyrrolyl and one η^1-pyrrolyl. Examination of the complex in solution by DOSY NMR suggests a solution state molecular weight intermediate to that of the monomer and the dimer. This may indicate that, in solution, fast equilibrium between the dimeric species and a smaller, monomeric species occurs. A species consistent with Ti(NHtolyl)$_2$(dpm) was not directly observed by ^{1}H NMR when **2^{tol}** was exposed to additional H_2Ntolyl, although it is likely that this bis(anilide) is present in some concentration.[59]

The ^{1}H NMR of dimer **2^{tol}** has quite broad resonances at room temperature related to the dpm ligand, which is likely due to rapid η^5- to η^1-exchange processes.[60] However, the ^{1}H NMR resonances for the tolyl-group are relatively sharp under the same conditions, indicative of a static Ti$_2$(N-*p*-tol)$_2$ core. Addition of excess *p*-toluidine did not noticeably perturb the ^{1}H NMR spectrum of the dimer. An additional DOSY experiment in the presence of excess *p*-toluidine gave very large errors in the diffusion constants, making the molecular weights for the monomer and dimer indistinguishable. Addition of isonitrile to dimer **2^{tol}** caused the dpm resonances to sharpen, suggesting the isonitrile interacts with the dimer to slow haptotropic rearrangement.

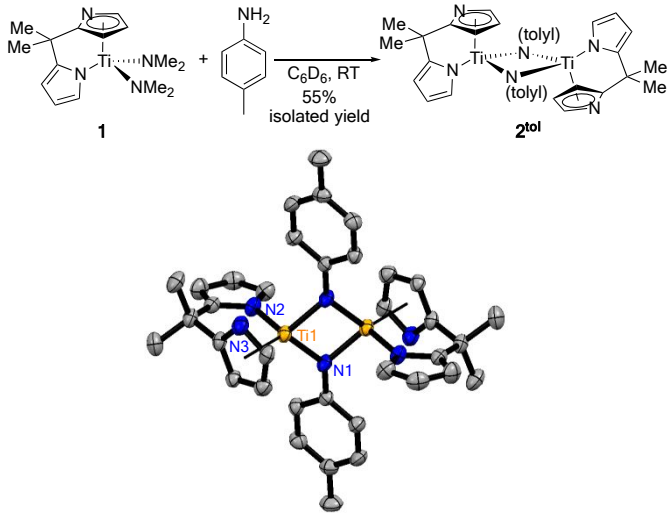

Figure 2. Synthesis of Ti(N-*p*-tol)(dpm)}$_2$ (**2^{tol}**) and structure from single crystal X-ray diffraction. Hydrogens in calculated positions are omitted and ellipsoids are at the 50% probability level. The molecule resides on a crystallographic inversion center.

The bridging imide **2^{Ph}**, similar to **2^{tol}** but with Ph replacing *p*-tolyl on the imide, was not directly observable under the catalytic conditions due to both the low catalyst concentration and the broad resonances of this species in the ^{1}H NMR due to the fluxionality previously discussed. However, we hypothesize that **2^{Ph}** is the resting state during the iminoamination catalysis shown in Table 1 because of its rapid formation and apparent stability. Another possibility for the resting state is an isonitrile-bound dimer or monomer, which has eluded characterization in our system thus far.

The resting state at low catalyst concentration and high amine concentration could also be the titanium bis(anilide) complex. However, as mentioned, aniline addition to **2^{tol}** does not lead to observable amounts of the bis(anilide) monomer, Ti(NHPh)$_2$(dpm), over the relative concentration range that we were able to examine by DOSY NMR. The bridging imide ligands in **2^{tol}** rapidly exchange with H_2NPh in solution, but the observed products show resonances in the ^{1}H NMR similar to the dimer, **2^{tol}**.

Unfortunately, the determination of the rate law for the titanium-catalyzed iminoamination reaction was more difficult than anticipated due to catalyst degradation involving the product (vide infra) and what may be changes in catalyst order with concentration. We hope to return to this issue and carry out additional mechanistic studies in subsequent work.

The dimer **2** is a catalyst for iminoamination, as would be expected. Using the conditions in Entry 3 with 5 mol% **1** gave 59% conversion after 19 h, and the same conditions with **2** (same mol% titanium) gave 57% conversion after 16 h. Consequently, their activities are very similar under these conditions.

The NMR resonances of the dimer **2** do not noticeably change in the presence of the iminoamination product in an otherwise pure solution; however, in the presence of isonitrile, **2^{tol}** reacts rapidly with the iminoamination product to give a plethora of unidentified compounds. Consistent with this catalyst degradation by product in iminoamination catalysis, using high catalyst loadings leads to observable loss of product at long reaction times. Consequently, this catalyst side reaction would seem to be dependent on the concentration of product, catalyst, and other compounds in solution but leads to decomposition.

In sum, there is a product-involved catalyst decomposition pathway that occurs relatively slowly compared to the productive catalytic reaction. Also, increasing the catalyst concentration may increase dimer formation potentially slowing the catalysis, and since the catalyst consumes the product via deactivation, higher catalyst concentrations can lead to lower yields. Consequently, there is much to be gained from carefully adjusting catalyst concentration in the reaction.

Since the active species is likely a monomeric imide with a low coordination number, we hypothesized that making the ancillary ligands on titanium more electron-rich would increase the reaction rate and improve performance, the rationale being that a more electron-rich metal center will have weaker bonds to the bridging imide and to other donor molecules in solution, e.g., isonitrile. Since only a small amount of the titanium is in the form of the active catalyst and most may be sitting as the dimer or other coordinated species, making the titanium center more electron-rich may increase the concentration of titanium

present as the presumed active species, the monomeric titanium imide.

As a more electron-rich system, we investigated the bidentate methylene bridged aryloxide **3** shown in Scheme 3, $Ti(NMe_2)_2(O_2Ar_2\text{-}6\text{-}CH_2)$ where Ar = 2-^{t}Bu-4-MeC_6H_2. Phenoxides, e.g., 4-methylphenoxide, generally have LDP values much lower (more donating) that pyrrolide, as can be seen in Figure 1. Consequently, **3** should have a significantly more electron-rich metal center than dpm-containing **1**.

Aryloxide **3** is readily prepared in 72% purified yield from $Ti(NMe_2)_4$ and $H_2O_2Ar_2\text{-}6\text{-}CH_2$, both of which are commercially available. It was found that reaction of **3** with H_2N-*p*-tolyl gave X-ray quality crystals of a dimeric complex in the solid state. Excitingly, and consistent with our expectations, the complex was a monomer in solution according to DOSY NMR, making it an excellent candidate for iminoamination catalysis.

Using the conditions in Entry 3 of Table 1 with **3** as catalyst gave nearly identical yield and reaction rate to $Ti(NMe_2)_2$(dpm) (**1**). The total yield for the reactions was comparable, while the initial rates were identical within the error of the experimental technique. (See the SI for a discussion of the initial rates in these reactions.)

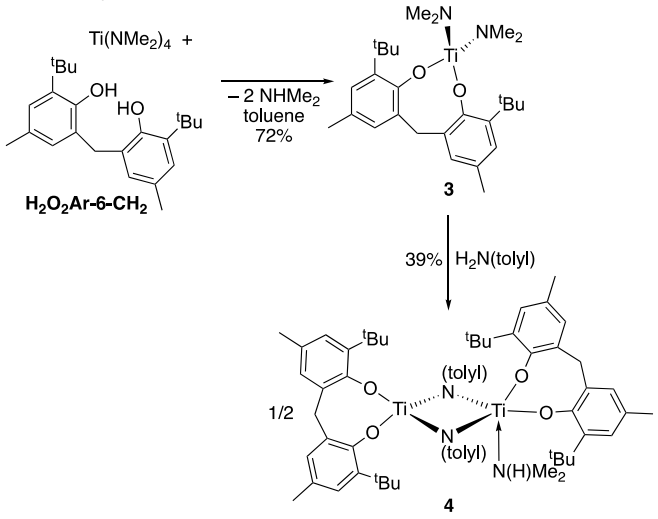

Scheme 3. Synthesis of $Ti(NMe_2)_2(O_2Ar_2\text{-}6\text{-}CH_2)$ (**3**) and the reaction of **3** with H_2N-*p*-tol to form the dimer $\{Ti(\mu\text{-}Ntolyl)_2(O_2Ar_2\text{-}6\text{-}CH_2)\}_2 \bullet HNMe_2$ (**4**), which was characterized by X-ray diffraction and has the structure shown in the line drawing. By DOSY NMR, **4** is a monomer in solution.

However, when the two catalysts were examined at higher concentrations, similar to those typically employed for the types of syntheses shown in Scheme 1, **3** demonstrated higher activity (Scheme 4). A reaction with 0.5 M each of H_2NPh, ^{t}BuNC, and 1-octyne with 5 mol % **3** provided 72% yield of the iminoamination product, 12% hydroamination, and 16% 4 component coupling (a 2,3-diaminopyrrole)[34] in 18 h with full conversion of the limiting reagent. The same reaction conditions with **1** provided only 65% iminoamination product and 10% HA with ~25% H_2NPh remaining after 24 h.

It is notable, also, that larger quantities of the 4CC product (2,3-diaminopyrrole) were generated in the reaction catalyzed by the more electron-rich **3** relative to **1**. This observation is consistent with previous studies from our group suggesting that more electron-rich ligands increase 4CC product formation.[34]

Interestingly, a new catalyst degradation pathway was noticed with these more electron-rich ancillary ligands, ligand disproportionation. Because of the readily observed, unique chemical shifts of **3** in the ^{1}H NMR spectrum due to the methylene bridge, an in situ iminoamination catalyzed by **3** was pursued. In this experiment, 20 mol % **3** (0.05 M) was used with H_2NPh, ^{t}BuNC, and 1-octyne (0.2 M each) in tol-d_8. After 16 h of heating at 110 °C, a new titanium complex was readily observed in solution. This complex was identified as $Ti(O_2Ar_2\text{-}6\text{-}CH_2)_2$ (**5**), Figure 3. Relative to ferrocene internal standard, **5** is present in 0.025 M concentration, thus this species represents half of the titanium and all of the bidentate aryloxide ligand added to the reaction mixture. The fate of the remaining titanium is not clear from the ^{1}H NMR of the crude reaction mixture, but presumably it bears a mixture of nitrogen-based ligands, e.g., anilide, imide, iminoamination product, etc. Evidence of disproportionation during the iminoamination reaction was not observed when using **1** as catalyst under similar conditions, i.e., no $Ti(dpm)_2$ was detected.

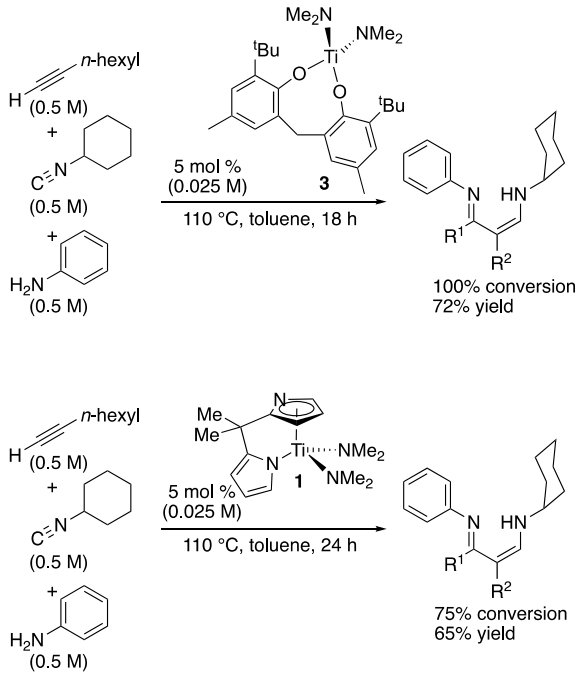

Scheme 4. Comparison of catalysts $Ti(NMe_2)_2(O_2Ar_2\text{-}6\text{-}CH_2)$ (**3**) and $Ti(NMe_2)_2$(dpm) (**1**). R^1 and R^2 are H or *n*-hexyl.

This finding makes it very challenging to effectively draw comparisons between catalytic reactions utilizing **1**, **3**, or other potential ancillary ligand candidates. The observation of **5** opens the possibility that precatalyst **3** is actually much more active than **1**, but the concentration of active catalyst is compromised by ligand disproportionation. The observation of ligand disproportionation in a catalytic reaction prompted the consideration of these processes in fundamental catalyst design, and the bigger question of why disproportion occurs with some ancillary ligands but not others within this system.

Modelling Equilibria of Heteroleptic Catalysts

In most catalytic cycles, the active species will be a heteroleptic complex with ancillary ligands that can be used to alter electronic structure and active sites for substrate transformation. Consequently, stability of heteroleptic complexes to disproportionation is a critical question for all catalyses as this can adversely affect the concentration of the active species. Can we predict, based on ligand properties, the outcome of equilibria involving catalytic species and if a catalyst architecture will be stable enough to provide high concentrations of the catalytically-active heteroleptic species?

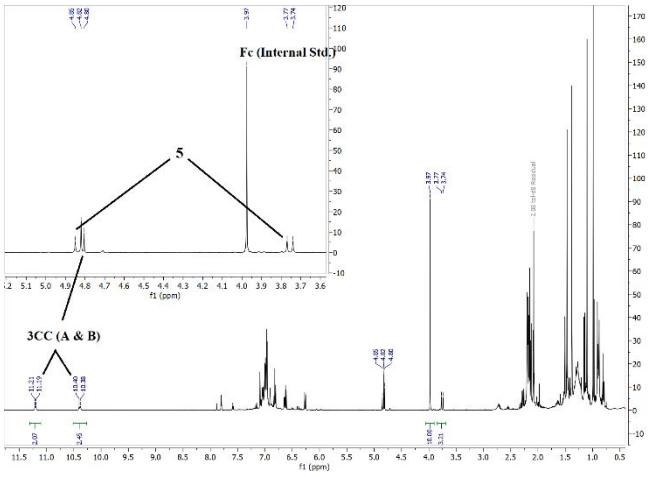

Figure 3. ^{1}H NMR spectrum of iminoamination of H_2NPh, ^{t}BuNC, and 1-octyne in tol-d_8 catalyzed by 20 mol% **3** at 110 °C for 16 h.

If one is studying ligand exchange in an A_2TiX_2 complex, there are 5 possible species in solution: TiX_4, $TiAX_3$, TiA_2X_2, TiA_3X, and TiA_4. In some cases, reactions can be driven to a single product. For example, $Ti(NMe_2)_4$ reacts with $TiCl_4$ in various stoichiometries to give a single heteroleptic product (Scheme 5).[61] Recall that chloride (LDP = 14.97 kcal/mol) and dimethylamide (LDP = 9.34) have very different donor abilities (Figure 1). Similarly, the heteroleptic complexes $TiCl_x(O^iPr)_{4-x}$ are all stable with ligands having very different donor abilities.[62]

$$3\ Ti(NMe_2)_4 + TiCl_4 \longrightarrow 4\ Ti(NMe_2)_3Cl$$

$$Ti(NMe_2)_4 + TiCl_4 \longrightarrow 2\ Ti(NMe_2)_2Cl_2$$

$$Ti(NMe_2)_4 + 3\ TiCl_4 \longrightarrow 4\ Ti(NMe_2)Cl_3$$

Scheme 5. Reaction of $Ti(NMe_2)_4$ and $TiCl_4$ can be used to cleanly prepare mixed $Ti(NMe_2)_xCl_{4-x}$ species by simply controlling the stoichiometry.

For relevance to our catalysis, which uses bidentate ancillary ligands, and also to simplify the reaction mixtures, we chose to study systems with at least one bidentate ligand on titanium. The bidentate ligand will be shown as $\{X_2\}$, where the brackets indicate the ligand is chelating and "X_2" indicates it is dianionic with two attachment sites to the metal. The hypothetical "X" ligand will have the same donor ability as ½ of the bis(phenoxide) ligand, $\{X_2\}$. The monodentate, monoanionic ligand will be "A".

It is important that the system lacks effects that would influence the equilibrium in some way other than the targeted electronic or steric effects rendered by the ligands under study. For example, the systems for study should not have a species that might precipitate or volatilize, which would change the equilibrium constant. Further, formation of stable dimers was to be avoided for this initial study, and we took some care to make sure all the species in the equilibria were monomeric in solution.

With the above in mind, we sought to answer a specific question: *does having ligands with very different donor abilities increase the stability of heteroleptic complexes towards disproportionation? If so, can we quantify the effect using LDP?*

In order to elucidate the effect of ligand donor abilities on the disproportionation equilibria, we decided to use the same chelating ligand in the catalyst $Ti(NMe_2)_2(O_2Ar_2\text{-}6\text{-}CH_2)$ (**3**), where Ar = 2-*tert*-butyl-4-methylphenol (Scheme 6) discussed earlier. The synthesis for the bischelate $Ti(O_2Ar_2\text{-}6\text{-}CH_2)_2$ (**5**) is shown in Scheme 4, which was prepared in 72% isolated yield by addition of commercially available $H_2O_2Ar_2\text{-}6\text{-}CH_2$ to **3**.

Also shown in Scheme 6 are the syntheses of the homoleptic tetra(aryloxide)titanium complexes (**6a-g**), which have a variety of different groups in the *para*-position of the aryloxide. These were accessed in good yields by addition of the substituted phenols to either $Ti(NMe_2)_4$ or $Ti(O^iPr)_4$.

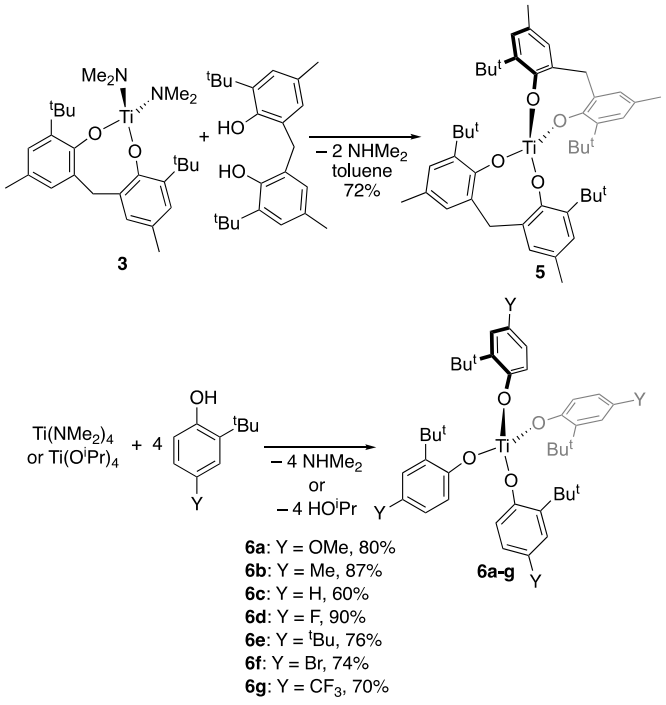

Scheme 6. Synthesis of $Ti(O_2Ar_2\text{-}6\text{-}CH_2)_2$ (**4**) and $Ti(OAr)_4$ (**6a-g**). In complexes **6**, the electronic structures was varied through a series of different groups Y in the *para*-position.

Bis(chelate) **5** could be added to homoleptic TiA_4 complexes, such as **6** in Scheme 6, to examine equilibria. This was particularly advantageous where A = aryloxide because the heteroleptic complexes, $Ti(OAr)_2(O_2Ar_2\text{-}6\text{-}CH_2)$, in this class could not be isolated in pure form due to disproportionation.

Other complexes where there is a larger difference in donor ability between X and A were isolable, e.g., **3**, and the equilibrium was started with the heteroleptic complexes $TiA_2(O_2Ar_2\text{-}6\text{-}CH_2)$.

The equilibrium constant, K_{eq}, is defined in the top portion of Figure 4 with larger equilibrium constants indicating that the heteroleptic complex is favored. In the bottom part of Figure 4, K_{eq} vs ΔLDP is plotted, where ΔLDP = (LDP of X) – (LDP of A). For the LDP of X, half of the chelating ligand, the value for 4-methylphenoxide was used (11.82 ± 0.1 kcal/mol); this introduced some error as will be discussed momentarily.

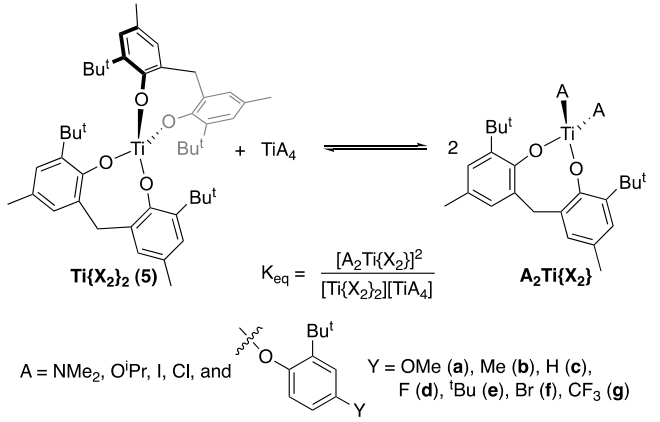

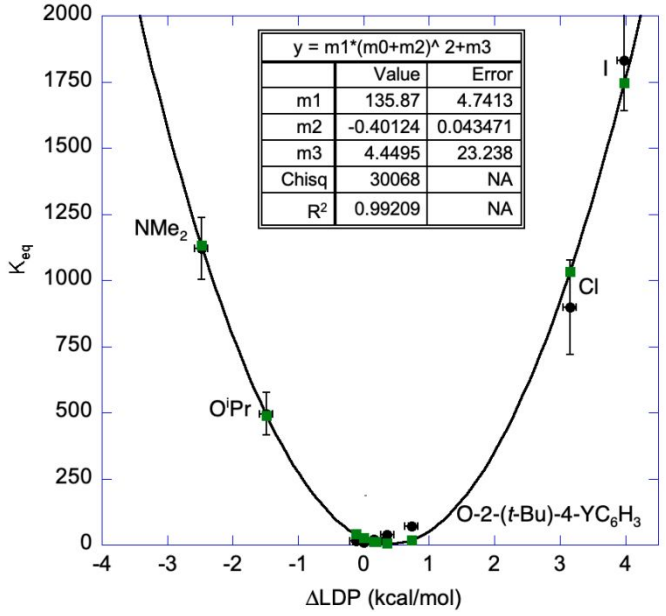

Figure 4. (*top*) The equilibria are defined with larger K_{eq} being observed when more heteroleptic complex is present. (*bottom*) Plot of K_{eq} vs ΔLDP. Black dots are the experimental data, and green dots (that are often overlapping) are from the model in Eq. 6. ΔLDP = (LDP of A) – (LDP of 4-MeC_4H_4O). The LDP of 4-MeC_4H_4O was used to approximate the donor ability of half of the chelating ligand. The error on LDP is estimated as 0.1 kcal/mol. The fit is drawn from a least square fit to the data (black points). The LDP value for OEt is being used for O^iPr. Most of the LDP values used can be found in Fig. 1; the values used for Y = ^{t}Bu, Br, and F were 12.01, 12.18, and 11.99, respectively.

As expected, what is observed is that, as A becomes significantly different from X in donor ability, the heteroleptic complex becomes more favored. In order to determine if the data could be fit to terms only involving the donor ability of the ligands, or if steric terms were also required, the data was modelled with and without steric terms.

A 5-parameter model was initially explored, which is shown in Eq. 1. The steric parameter used was percent buried volume, $\%V_{bur}$, developed by Cavallo and coworkers, which employed the structures of the titanium complexes from X-ray diffraction.[63, 64] Percent buried volume was quite useful in our previous studies modelling titanium reactions.[54]

$$K_{eq} = a + b(\Delta LDP) + c(\Delta LDP)^2 + d(\%V_{bur}) + e(\%V_{bur})^2 \quad (1)$$

Using Eq. 1, the coefficients for the steric parameters were significantly smaller than those for the electronic terms. In addition, the average errors from the experimental values for K_{eq} were smaller if the steric terms were dropped. Consequently, it doesn't appear that steric terms are important for understanding the equilibrium behavior for the ligand sets examined here. A 4-parameter model, using the terms in Eq. 1 with *a-d* coefficients, did not yield improvements over simply using the electronic terms either.

The simple model shown in Eq. 2 was used instead.

$$K_{eq} = a + b(\Delta LDP) + c(\Delta LDP)^2 \quad (2)$$

From the least squares fit (see the SI), the coefficients *a, b*, and *c* were found to be as shown in Eq. 3.

$$K_{eq} = 22 - 98(\Delta LDP) + 136(\Delta LDP)^2 \quad (3)$$

Eq. 3 is a quadratic that can to rewritten in the vertex form for a parabolic equation, which is more meaningful in this case. The vertex form of the equation is shown in Eq. 4.[§]

$$K_{eq} = 136(\Delta LDP - 0.36)^2 + 4.3 \quad (4)$$

The assumption here is that the vertex of the parabola should be where the donor abilities of A and X are equal, i.e., where the "real" ΔLDP is zero. However, the LDP system is designed to give values for monodentate ligands that are relatively small, and we can't directly measure the donor ability of the bisphenoxide chelate. Here, as mentioned, we are using the LDP of 4-methylphenoxide (11.82) as the value for half of the chelate, X; this is because placing groups in the 2-position of the phenol causes steric interference in the LDP measurement. From the parameters in Eq. 4, the actual value of LDP for the hypothetical ligand X (one-half of the chelate) can be calculated as 11.82 – 0.36 = 11.46. In other words, addition of a 2-*tert*-butyl group and the linker in the 6-position, lowers (more donating) the LDP of 4-methylphenoxide by 0.36 kcal/mol.[‡]

Eq. 4 was used to generate the model points in Figure 4. In the figure, the model was used to calculate the green boxes for each ligand, A, and the experimentally-measured equilibrium constants were shown as black dots. The curve in this figure was determined from an iterative least square fit, which gave almost identical results; compare the parameters in Figure 4 with Eq. 4 and the curve with the location of the green boxes.

Concluding Remarks

A study of the reaction of a common catalyst for iminoamination, dipyrrolylmethane-containing **1**, showed that the complex rapidly reacts with *p*-tolylamine to generate the dimeric μ-imido complex $\mathbf{2^{tol}}$. Unfortunately, the complex shows broad resonances in the ^{1}H NMR, which make it

somewhat difficult to identify in reaction mixtures; however, we postulate that this dimeric complex is possibly the resting state of the catalyst during iminoamination reactions. The dimeric μ-imido complex **2^{tol}** rapidly reacts with aniline, and presumably other primary amines, to exchange the imide ligand.

It was found that **2^{tol}** reacts with *tert*-butylisonitrile in solution in a fashion that leads to sharpening of the dpm resonances in the ^{1}H NMR. The slowing of the exchange of the pyrrolyl groups is likely due to coordination of isonitrile to the metal center; however, this isonitrile-coordinated species has not been isolated. Importantly, **2** does not seem to react with the iminoamination product in pure solution, but rapid decomposition was observed when **2** was treated with iminoamination product in the presence of isonitrile. In other words, it appears that the catalyst is unstable in the presence of product under the reaction conditions. The decomposition is relatively slow under the catalytic conditions considering the reactions can be run to relatively high yields in some cases; however, this reaction between catalyst and product is perhaps a critical one to understand and consider when attempting to improve catalyst performance in the future. Further, decomposition of the product is noticeable at high catalyst loadings towards the end of the reaction.

Working under the assumption that the active species in the catalytic reaction is a low-coordinate, monomeric titanium imide, it was hypothesized that making the ancillary ligand more electron-rich would destabilize the dimer and discourage coordination of other potential donors in solution. Consequently, an aryloxide-based precatalyst, **3**, was investigated, which should be more electron-rich than pyrrolyl-containing **1**.

Under some conditions, aryloxide-containing **3** (Scheme 4) is in fact faster than **1** for iminoamination. However, there is a new complication with the more electron-rich system. It was observed that the catalyst undergoes disproportionation under catalytic conditions to generate $Ti(NMe_2)_4$ and bis(chelate)titanium **5**, neither of which are catalytically active for iminoamination under the reaction conditions here. As a result, the catalyst concentration is reduced by this disproportionation. To understand this catalyst deactivation in more detail, we carried out a study on titanium disproportionation and the factors controlling it in a titanium system.

It was found that ligand exchange is encouraged in heteroleptic complexes where the ligands are similar in donor ability. With these parameterization methods in place, one can begin to anticipate the stability of heteroleptic titanium catalysts toward disproportionation. For example, while catalyst **3** with aryloxide (LDP = 11.40) and dimethylamide (LDP = 9.34) is susceptible to disproportionation with a K_{eq} of 1120 ± 118, catalyst **1** with pyrrolyl (LDP ~ 13.64) and dimethylamide (LDP = 9.34) ligands does not undergo disproportionation to any extent that we could observe experimentally. From Eq. 4, one can calculate that K_{eq} for **1** should be ~2100, which is higher than the largest equilibrium constant we were able to measure by ^{1}H NMR in this study (1830 for A = iodide). Therefore, consideration of the predicted K_{eq} values for ancillary ligand candidates for use in the titanium-catalyzed iminoamination reaction may direct efforts to find a faster catalyst that avoids the instability of ligand disproportionation.

The coefficients in Eq. 4 in some cases might be related to properties of the metal or, at least, properties dependent on the metal center. The coefficient in front of the squared parenthetical term gives the change in K_{eq} relative to ΔLDP^2. The larger this coefficient, the steeper the parabolic curve, and the larger the change in K_{eq} with unit changes in ΔLDP^2. The constant within the parentheses, –0.36, is simply correcting our zero of ΔLDP, which we can't measure directly for hypothetical ligand X (one-half of the chelating ligand).§

Do the shapes of these parabolas change with the nature of the metal center, e.g., will zirconium give a narrower (or wider) parabola with larger (or smaller) changes in K_{eq} with unit changes in ΔLDP^2? One can wonder if venerable ideas like the Hard-Soft Acid-Base principle[65-68] will be a useful guide for these explorations or if a different framework is necessary to understand these fundamental processes of reaction chemistry.

Not studied here in detail, the kinetics of disproportionation may be just as critical to catalytic applications of heteroleptic complexes. The sterics were not found to be of great importance to equilibria of heteroleptic titanium complexes in this case. However, we did not thoroughly explore the rate to reach equilibrium, which may have a steric component. Obviously, catalysts that are thermodynamically unstable to disproportionation, may be quite useful if disproportionation is much slower than the catalysis of interest.

Finally, the methods explored here for studying ligand exchange in heteroleptic titanium complexes suggest that some systems should be carefully vetted for disproportionation, especially in cases where the precatalyst, or long-lived complexes in the catalytic mixture, have ligands on the metal with similar donor abilities. In some cases, it may be necessary to explore methods for discouraging bimolecular ligand exchange in catalysts, which may be done with strategic use of steric blocking in some cases. Another approach to discourage ligand disproportionation is to move to heterogeneous catalysts, which we are currently exploring for these reactions.[32]

Experimental

General Considerations

Routine characterization spectra were obtained using an Agilent DDR2 500 MHz NMR spectrometer equipped with a 5 mm PFG OneProbe operating at 499.84 MHz (^{1}H) and 125.73 MHz (^{13}C). ^{1}H NMR chemical shifts were referenced to residual $CHCl_3$ in $CDCl_3$ as 7.26 ppm or residual C_6HD_5 in C_6D_6 as 7.16 ppm. ^{13}C NMR chemical shifts are reported relative to $^{13}CDCl_3$ as 77.16 ppm, or (^{13}C)C_5D_6 as 128.06 ppm. The Varian Dbppste_cc (DOSY bipolar pulse pair simulated spin echo convection corrected) pulse sequence was utilized for all experiments where DOSY NMR was used. All spectra were multiplied by a weighted exponential of 10 Hz and baseline corrected before applying DOSY processing. Standard DOSY processing, as

supplied by the vendor, was used based on peak heights and with compensation for non-uniform gradients. For notes on NMR-based determination of K_{eq}, see below.

GCMS data was collected on an Agilent 5973 MSD with a 6890N series GC. GCFID data was collected on a Hewlett Packard 6890 series GC system and standardized against dodecane as an internal standard. Iminoamination products were quantified *in situ* by utilizing GCFID standardized calibration curves generated by quantification of the authentic iminoamination product, isolated from a catalytic reaction mixture. The HA and 4CC products were quantified analogously to the iminoamination product. More details can be found in the SI.

All single crystal X-ray structures were collected at the MSU Center for Crystallographic Research. The data was collected on Bruker diffractometers running either Mo or Cu-Kα radiation. The collection data and information about the unit cell, etc. for these structures can be found in the .cif files for each structure.

All manipulations were carried out under inert atmosphere, either in an N_2 atmosphere MBraun glovebox or utilizing standard Schlenk techniques. The only bench-top manipulations were those to prepare materials for use in the glovebox and isolation of air-stable organic compounds.

The solvents toluene, pentanes, and Et_2O were dried over activated alumina and sparged with N_2 prior to use. *n*-Hexane was dried over sodium and distilled under N_2 prior to use. C_6D_6 was purchased from Sigma-Aldrich. Toluene-d_8 was purchased from Cambridge Isotopes. Toluene-d_8 and benzene-d_6 were dried over CaH_2 and distilled under N_2, then stored in the dry box on 3 Å molecular sieves prior to use. $CDCl_3$ was purchased from Cambridge Isotopes and was used as received for characterization of organic products. For use with titanium complexes, the $CDCl_3$ was dried over P_2O_5 and distilled under N_2 prior to use; the dry $CDCl_3$ was stored in a glovebox under an inert atmosphere. Additional solvents, including those used for column chromatography (hexanes, EtOAc, etc.), were used as received.

The aryloxides 2-*tert*-butylphenoxide, 4-bromomphenol, 4-fluorophenol, 2,4-di-*tert*-butylphenol, 2-*tert*-butyl-4-methylphenol, and 2-*tert*-butyl-4-methoxyphenol were purchased from Sigma-Aldrich. A 2-*tert*-butyl group was added to 4-bromophenol and 4-fluorophenol using the literature procedure.[69] The starting material 4-trifluoromethylphenol was purchased from Sigma-Aldrich and a 2-*tert*-butyl was added to the ring using the literature procedure.[70] The bischelate 2,2'-methylene-*bis*(6-*tert*-butyl-4-methylphenol) was purchased from Sigma-Aldrich. The phenols were purified by either sublimation or azeotropic elimination of water with benzene using a Dean-Stark apparatus.

Aniline was purchased from Alfa Aesar, was dried over CaH_2, and was distillled under reduced pressure. *Tert*-butylisonitrile was prepared according to literature procedures.[71] 1-octyne was purchased from Alfa Aesar, was dried over anhydrous sodium sulfate, was distilled under N_2, and then was stored under an inert atmosphere over 3 Å molecular sieves. TiO^iPr_4 and $TiCl_4$ were purchased from Sigma-Aldrich and used as received. Trimethyliodosilane stored over Cu^0 was purchased from Gelest and used as received. Tetrakis(trimethylsilyl)silane was purchased from Gelest and used as received. Ferrocene was purchased from Strem Chemical and was sublimed prior to use.

$Ti(NMe_2)_4$ was purchased from Gelest and used as received. $Ti(dpm)(NMe_2)_2$ was prepared according to literature procedure.[72] $Ti(O_2Ar_2\text{-}6\text{-}CH_2)Cl_2$ and $Ti(O_2Ar_2\text{-}6\text{-}CH_2)I_2$ were prepared using the literature procedures.[73]

General Procedure for the Synthesis of $Ti(OAr)_4$ (6)

The tetra(aryloxide)titanium complexes were prepared using similar procedures with either $Ti(NMe_2)_4$ or $Ti(O^iPr)_4$ as the starting material. The synthesis of tetrakis(2,4-di-*tert*-butyl-phenoxide)titanium(IV) (**6e**) is given here as an example; see the SI for details on other derivatives. A scintillation vial was charged with $Ti(NMe_2)_4$ (200 mg, 0.89 mmol, 1 equiv), a stir bar, and *n*-hexane (5 mL). The vial was chilled in a cold well cooled with liquid N_2 for 20 min, until the hexane solution was frozen. The vial was warmed ambiently, with stirring, until the solution was just thawed, and a toluene (2 mL) solution of 2,4-di-tert-butylphenol (732 mg, 3.6 mmol, 4 equiv) was added dropwise. The pale-yellow solution rapidly turned bright orange. This solution was stirred for 2 h at room temperature, and the volatiles were removed in vacuo to yield an orange powder. The powder was rinsed with hexane and dried. The residue was dissolved in a minimal amount of toluene, and the concentrated solution was stored at –35 °C overnight to yield X-ray quality crystals of **6e** (589 mg, 76%). ^{1}H NMR (500 MHz, benzene-d_6): 7.47 (d, J = 2.4 Hz, 4H), 7.42 (d, J = 8.3 Hz, 4H), 6.95 (dd, J = 8.3, 2.4 Hz, 4H), 1.60 (s, 36H), 1.21 (s, 36H).^{13}C NMR (126 MHz, benzene-d_6): 162.29, 145.41, 135.96, 124.70, 123.67, 122.98, 35.43, 34.63, 31.70, 30.57. Elemental Analysis calc. for $C_{56}H_{84}O_4Ti$: C, 77.39; H, 9.74; N, 0.0. Found: C, 76.97; H, 9.46; N, 0.10.

Synthesis of $Ti(NMe_2)_2(O_2Ar_2\text{-}6\text{-}CH_2)$ (3)

$Ti(NMe_2)_2(O_2Ar_2\text{-}6\text{-}CH_2)$ (**3**) has been previously reported;[74] however, we used a different protocol. A scintillation vial was charged with $Ti(NMe_2)_4$ (400 mg, 1.8 mmol), a stir bar, and toluene (10 mL). Separately, a solution containing HO2Ar2-6-CH2H (610 mg, 1.8 mmol) and toluene (4 mL) was prepared. The ligand solution was then added to the $Ti(NMe_2)_4$ solution dropwise with stirring. The pale-yellow solution gradually darkened and turned orange. The solution was stirred for 4 h at room temperature, and the volatiles were removed in vacuo to yield an orange oil. Repeatedly, the orange oil was tritrated with pentanes (3 mL x 4) and volatiles were removed in vacuo to obtain a foam. The foam was dissolved in a minimal amount of pentanes or n-hexane, and **3** precipitated as a yellow-orange powder (614 mg, 72%). The ^{1}H and ^{13}C NMR spectroscopy of **3** matched literature values.[74]

Synthesis of $Ti(O^iPr)_2(O_2Ar_2\text{-}6\text{-}CH_2)$

$Ti(O^iPr)_2(O_2Ar_2\text{-}6\text{-}CH_2)$ has been previously reported, and a slightly modified procedure was used.[73] A scintillation vial was charged with $Ti(O^iPr)_4$ (145 mg, 0.51 mmol), a stir bar, and DCM (4 mL). A solution of $H_2(O_2Ar_2\text{-}6\text{-}CH_2)$ (172 mg, 0.51 mmol) in DCM (2 mL) was prepared, which was added dropwise with stirring to the $Ti(O^iPr)_4$ solution at room temperature. The

solution rapidly went from colorless to orange. Stirring was continued at room temperature for 4 h. Over this time, an orange precipitate formed. The solution was decanted, and the solid product was dried in vacuo. To isolate additional product, the decanted solution was layered with *n*-hexane and chilled to –35 °C, which resulted in powder and X-ray quality single crystals. In total, 210 mg (82%) of product was isolated. The ^{1}H and ^{13}C NMR spectroscopy of the product matched literature values.[73]

Synthesis of Ti(O_2Ar_2-6-CH_2)$_2$ (5)

5 has been previously reported, and a slightly modified procedure was used.[73] A scintillation vial was charged with Ti(O_2Ar_2-6-CH_2)(NMe_2)$_2$ (**3**) (200 mg, 0.42 mmol), a stir bar, and toluene (4 mL). A toluene (2 mL) solution of H(O_2Ar_2-6-CH_2)H (143 mg, 0.42 mmol) was added dropwise to the stirred solution of **3** at room temperature. The orange solution darkened slightly during addition. In total, the solution was stirred for 2 h at room temperature The volatiles were removed in vacuo, and an orange residue was obtained. Repeatedly, the residue was tritrated with pentanes (3 mL x 4) and the volatiles were removed in vacuo until a yellow foam was obtained. With this foam, **5** (189 mg, 62%) was obtained as X-ray quality crystals from a concentrated *n*-hexane solution stored at -35 °C. The ^{1}H and ^{13}C NMR spectroscopy of **5** matched literature reports.[73]

Synthesis of {Ti(dpm)(μ-Ntolyl)}$_2$ (2^{tol})

To a stirred, room temperature solution of Ti(dpm)(NMe_2)$_2$ (**1**) (50 mg, 1 equiv) in C_6D_6 (1.5 mL) was added a solution of H_2Ntolyl (34 mg, 2 equiv) in of C_6D_6 (0.5 mL). The solution darkened from light yellow to dark reddish-brown. The solution was stirred for 10 min at room temperature and was then examined by ^{1}H NMR spectroscopy. The spectrum showed that one equivalent of H_2Ntolyl reacted with **1** while one equivalent remained free in solution. Integral values for the new species were consistent with a 1:1 ratio of dpm to tolyl groups. There was fluxionality within the complex at room temperature, evidenced by broad resonances in the ^{1}H NMR. X-ray quality crystals were grown from toluene/*n*-hexane at –35 °C. The compound **2**^{tol} (30 mg, 58%) also could be purified from Et_2O/*n*-hexane at –35 °C. NMR investigations of isolated single crystals of **2^{tol}** also showed broad resonances in the ^{1}H NMR at room temperature due to rapid haptotropic shifting of the η^1/η^5-pyrrole rings in the dpm ligands that begin to resolve around –75 °C. ^{1}H NMR (500 MHz, tol-d_8, –75 °C): 7.63 (s, 2H), 6.76 (d, *J* = 8.5 Hz, 2H), 6.53 (s, 1H), 6.44 (s, 2H), 6.36 (m, 6H), 6.06 (d, *J* = 6.2 Hz, 2H), 5.82 (s, 2H), 5.65 (s, 1H), 1.97 (d, *J* = 17.6 Hz) and 1.93 (s, 13H), 1.58 (d, *J* = 17.4 Hz, 6H). ^{13}C NMR (126 MHz, tol-d_8, –75 °C): 173.05, 170.55, 158.50, 157.34, 127.15, 126.84, 125.90, 124.54, 122.32, 113.80, 108.45, 45.38, 39.86, 28.70, 28.45. UV-vis, λ_{max}: 480 nm (ε = 2503 $M^{-1}cm^{-1}$), 335 nm (ε = 7105 $M^{-1}cm^{-1}$). Note, repeated attempts to obtain passing elemental analysis failed to yield adequate results.

Synthesis of {Ti(O_2Ar_2-6-CH_2)(μ-Ntolyl)}$_2$•$HNMe_2$ (4)

A scintillation vial was charged with Ti(O_2Ar_2-6-CH_2)(NMe_2)$_2$ (**3**) (100 mg, 0.21 mmol, 1 equiv), a stir bar, and benzene (2 mL). A separate solution of H_2Ntolyl (23 mg, 0.21 mmol, 1 equiv) was prepared in benzene (1 mL). The H_2Ntolyl solution was added dropwise to the stirred solution of **3**, which resulted in a color change from yellow-orange to dark reddish-brown. The solution was stirred for 1 h at room temperature, and the volatiles were removed in vacuo, which provided a dark-brown powder. X-ray quality crystals were obtained from a concentrated solutionin *n*-hexane at –35 °C, that were found to be [Ti(O_2Ar_2-6-CH_2)(μ-Ntolyl)]$_2$•$NHMe_2$ (**4**) (39%, 41 mg). Based on DOSY analysis, it appears that this dimer is monomeric in solution at room temperature. ^{1}H NMR (500 MHz, benzene-d_6): 7.06-6.98 (m, 12H), 6.80 (d, *J* = 7.8 Hz, 4H), 3.80 (d, *J* = 14.2 Hz, 2H), 3.36 (d, *J* = 14.3 Hz, 2H), 2.15 (s, 12H), 2.01 (s, 6H), 1.79 (s, 5 H), 1.66 (s, 36H).^{13}C NMR (126 MHz, benzene-d_6): 161.02, 136.29, 132.93, 130.26, 129.65, 129.37, 126.11, 121.40, 40.30, 31.30, 21.19, 20.81. Elemental Analysis calc. for $C_{62}H_{81}O_4N_3Ti_2$: C, 72.43; H, 7.94; N, 4.09. Found: C, 72.00; H, 8.35; N, 3.56.

Measurement of Equilibria

The determination of the K_{eq} values for the ligand exchange reactions, were performed by monitoring the concentrations of the 3 species in solution (Fig. 4) by ^{1}H NMR. Solutions (0.025-0.05 M in titanium complexes) were prepared in C_6D_6. Ferrocene (~0.03 M) was included as an internal standard. Due to the long T_1 of ferrocene (~30 s) in deoxygenated NMR solvents, the NMR experiments were performed with d1 = 150 and gain = 30 for accurate quantitation. The solutions were examined every few days until the integral values of the species in solution had stopped changing. Once the solution concentrations of the species of interest had stopped changing, 3 spectra were taken and averaged. From these triplicate measurements, an error could be assigned to K_{eq}, which is largely based on integration error in the ^{1}H NMR. For A = I, Cl, O^{i}Pr, and NMe_2, the equilibrium processes were initiated from Ti(A)$_2$(O2Ar2-6-CH2). The Ti(OAr)$_2$(O_2Ar_2-6-CH_2) species typically begin ligand exchange processes while trying to isolate these heteroleptic species from the crude reaction mixture and therefore could not be isolated in pure form. For the ligand exchange reactions with the various 2-*tert*-butyl-4-R-phenoxide ligands, the equilibrium exchange process was initiated from the two homoleptic species Ti(OAr)$_4$ (**6**) and Ti(O_2Ar_2-6-CH_2)$_2$ (**5**) added in equivalent molar amounts to the initial solution.

Conflicts of interest

There are no conflicts to declare.

Acknowledgements

KEA thanks the American Association of University Women for funding during the 2018-2019 academic year through a Dissertation Completion Fellowship. We greatly appreciate the financial support of the National Science Foundation through CHE-1562140.

Notes and references

‡ Some error is introduced for the monodentate aryloxides due to limitations in experimentally determining LDP values. For the

donor abilities of the 2-^{t}Bu-4-Y-phenoxides ligands, the LDP values for 4-Y-phenoxides were used because the 2-^{t}Bu-group sterically inhibits amide rotation in the chromium system, as does a 2-Me-group.

§ The last term (+0.35) in Eq. 4 gives the value of K_{eq} when the equation is at ΔLDP = 0, which one might expect to be ~1. A least square fit (Figure 4) to the data including this term gave a value of 4 ± 23, i.e., the value is insignificant relative to the error. This simply suggests that perhaps K_{eq} ~ 1 when the ligands involved are equal donors. Dropping the parameter induces negligible error in the fit, but it was retained here for completeness.

1. Y. Gao, R. M. Hanson, J. M. Klunder, S. Y. Ko, H. Masamune and K. B. Sharpless, *J. Am. Chem. Soc.*, 1987, **109**, 5765-5780.
2. T. Katsuki and K. B. Sharpless, *J. Am. Chem. Soc.*, 1980, **102**, 5974-5976.
3. H. C. Kolb, M. S. Vannieuwenhze and K. B. Sharpless, *Chem. Rev.*, 1994, **94**, 2483-2547.
4. K. B. Sharpless, *Angew. Chem. Int. Ed.*, 2002, **41**, 2024-2032.
5. K. B. Sharpless, W. Amberg, Y. L. Bennani, G. A. Crispino, J. Hartung, K. S. Jeong, H. L. Kwong, K. Morikawa, Z. M. Wang, D. Q. Xu and X. L. Zhang, *J. Org. Chem.*, 1992, **57**, 2768-2771.
6. I. Marek, *Titanium and Zirconium in Organic Synthesis*, Wiley-VCH, Weinheim, 2002.
7. H. H. Brintzinger, D. Fischer, R. Mulhaupt, B. Rieger and R. M. Waymouth, *Angew. Chem. Int. Ed.*, 1995, **34**, 1143-1170.
8. J. D. Scollard and D. H. McConville, *J. Am. Chem. Soc.*, 1996, **118**, 10008-10009.
9. S. G. Feng, J. Klosin, W. J. Kruper, M. H. McAdon, D. R. Neithamer, P. N. Nickias, J. T. Patton, D. R. Wilson, K. A. Abboud and C. L. Stern, *Organometallics*, 1999, **18**, 1159-1167.
10. H. G. Alt and A. Koppl, *Chem. Rev.*, 2000, **100**, 1205-1221.
11. E. Y. X. Chen and T. J. Marks, *Chem. Rev.*, 2000, **100**, 1391-1434.
12. G. J. Domski, J. M. Rose, G. W. Coates, A. D. Bolig and M. Brookhart, *Prog. Polym. Sci.*, 2007, **32**, 30-92.
13. L. Bareille, P. Le Gendre and C. Moise, *Chem. Commun.*, 2005, 775-777.
14. J. A. Bexrud, P. Eisenberger, D. C. Leitch, P. R. Payne and L. L. Schafer, *J. Am. Chem. Soc.*, 2009, **131**, 2116-+.
15. E. Chong, P. Garcia and L. L. Schafer, *Synthesis-Stuttgart*, 2014, **46**, 2884-2896.
16. P. Eisenberger, R. O. Ayinla, J. M. P. Lauzon and L. L. Schafer, *Angew. Chem. Int. Ed.*, 2009, **48**, 8361-8365.
17. P. Garcia, Y. Y. Lau, M. R. Perry and L. L. Schafer, *Angew. Chem. Int. Ed.*, 2013, **52**, 9144-9148.
18. J. Hannedouche and E. Schulz, *Organometallics*, 2018, **37**, 4313-4326.
19. S. B. Herzon and J. F. Hartwig, *J. Am. Chem. Soc.*, 2007, **129**, 6690.
20. S. B. Herzon and J. F. Hartwig, *J. Am. Chem. Soc.*, 2008, **130**, 14940.
21. K. Krueger, A. Tillack and M. Beller, *ChemSusChem*, 2009, **2**, 715-717.
22. R. Kubiak, I. Prochnow and S. Doye, *Angew. Chem. Int. Ed.*, 2009, **48**, 1153-1156.
23. R. Kubiak, I. Prochnow and S. Doye, *Angew. Chem. Int. Ed.*, 2010, **49**, 2626-2629.
24. M. Manssen, N. Lauterbach, J. Doerfler, M. Schmidtmann, W. Saak, S. Doye and R. Beckhaus, *Angew. Chem. Int. Ed.*, 2015, **54**, 4383-4387.
25. T. Preuss, W. Saak and S. Doye, *Chem. Eur. J.*, 2013, **19**, 3833-3837.
26. I. Prochnow, P. Zark, T. Mueller and S. Doye, *Angew. Chem. Int. Ed.*, 2011, **50**, 6401-6405.
27. A. L. Reznichenko, T. J. Emge, S. Audoersch, E. G. Klauber, K. C. Hultzsch and B. Schmidt, *Organometallics*, 2011, **30**, 921-924.
28. A. L. Reznichenko and K. C. Hultzsch, *J. Am. Chem. Soc.*, 2012, **134**, 3300-3311.
29. P. W. Roesky, *Angew. Chem. Int. Ed.*, 2009, **48**, 4892-4894.
30. S. A. Ryken and L. L. Schafer, *Acc. Chem. Res.*, 2015, **48**, 2576-2586.
31. G. Zi, F. Zhang and H. Song, *Chem. Commun.*, 2010, **46**, 6296-6298.
32. K. E. Aldrich and A. L. Odom, *Organometallics*, 2018, **37**, 4341-4349.
33. S. Banerjee, Y. H. Shi, C. S. Cao and A. L. Odom, *J. Organomet. Chem.*, 2005, **690**, 5066-5077.
34. E. Barnea, S. Majumder, R. J. Staples and A. L. Odom, *Organometallics*, 2009, **28**, 3876-3881.
35. C. S. Cao, Y. H. Shi and A. L. Odom, *J. Am. Chem. Soc.*, 2003, **125**, 2880-2881.
36. H.-C. Chiu and I. A. Tonks, *Angew. Chem. Int. Ed.*, 2018, **57**, 6090-6094.
37. Z. W. Davis-Gilbert and I. A. Tonks, *Dalton Trans.*, 2017, **46**, 11522-11528.
38. Z. W. Davis-Gilbert, X. Wen, J. D. Goodpaster and I. A. Tonks, *J. Am. Chem. Soc.*, 2018, **140**, 7267-7281.
39. Z. W. Davis-Gilbert, L. J. Yao and I. A. Tonks, *J. Am. Chem. Soc.*, 2016, **138**, 14570-14573.
40. A. A. Dissanayake and A. L. Odom, *Tetrahedron*, 2012, **68**, 807-812.
41. A. A. Dissanayake, R. J. Staples and A. L. Odom, *Adv. Synth. Catal.*, 2014, **356**, 1811-1822.
42. Z. W. Gilbert, R. J. Hue and I. A. Tonks, *Nature Chem.*, 2016, **8**, 63-68.
43. S. Majumder, K. R. Gipson and A. L. Odom, *Org. Lett.*, 2009, **11**, 4720-4723.
44. S. Majumder, K. R. Gipson, R. J. Staples and A. L. Odom, *Adv. Synth. Catal.*, 2009, **351**, 2013-2023.
45. S. Majumder and A. L. Odom, *Tetrahedron*, 2010, **66**, 3152-3158.
46. T. J. McDaniel, T. A. Lansdell, A. A. Dissanayake, L. M. Azevedo, J. Claes, A. L. Odom and J. J. Tepe, *Biorg. Med. Chem.*, 2016, **24**, 2441-2450.
47. A. L. Odom, *Dalton Trans.*, 2005, DOI: 10.1039/b415701j, 225-233.
48. A. L. Odom and T. J. McDaniel, *Acc. Chem. Res.*, 2015, **48**, 2822-2833.
49. C. M. Pasko, A. A. Dissanayake, B. S. Billow and A. L. Odom, *Tetrahedron*, 2016, **72**, 1168-1176.
50. C. A. Tolman, *Chem. Rev.*, 1977, **77**, 313-348.
51. S. A. DiFranco, N. A. Maciulis, R. J. Staples, R. J. Batrice and A. L. Odom, *Inorg. Chem.*, 2012, **51**, 1187-1200.
52. K. E. Aldrich, B. S. Billow, R. J. Staples and A. L. Odom, *Polyhedron*, 2019, **159**, 284-297.
53. R. D. Bemowski, A. K. Singh, B. J. Bajorek, Y. DePorre and A. L. Odom, *Dalton Trans.*, 2014, **43**, 12299-12305.

54. B. S. Billow, T. J. McDaniel and A. L. Odom, *Nature Chem.*, 2017, **9**, 837-842.
55. K. E. Aldrich, B. S. Billow, D. Holmes, R. D. Bemowski and A. L. Odom, *Organometallics*, 2017, **36**, 1227-1237.
56. B. S. Billow, R. D. Bemowski, S. A. DiFranco, R. J. Staples and A. L. Odom, *Organometallics*, 2015, **34**, 4567-4573.
57. S. Banerjee and A. L. Odom, *Organometallics*, 2006, **25**, 3099-2006.
58. N. Vujkovic, J. L. Fillol, B. D. Ward, H. Wadepohl, P. Mountford and L. H. Gade, *Organometallics*, 2008, **27**, 2518-2528.
59. P. J. Walsh, A. M. Baranger and R. G. Bergman, *J. Am. Chem. Soc.*, 1992, **114**, 1708-1719.
60. D. L. Swartz, II and A. L. Odom, *Dalton Trans.*, 2008, 4254-4258.
61. E. Benzing and W. Kornicker, *Chem. Ber. Recl.*, 1961, **94**, 2263-2267.
62. M. Kamigaito, M. Sawamoto and T. Higashimura, *Macromolecules*, 1995, **28**, 5671-5675.
63. L. Falivene, R. Credendino, A. Poater, A. Petta, L. Serra, R. Oliva, V. Scarano and L. Cavallo, *Organometallics*, 2016, **35**, 2286-2293.
64. A. Poater, B. Cosenza, A. Correa, S. Giudice, F. Ragone, V. Scarano and L. Cavallo, *Eur. J. Inorg. Chem.*, 2009, 1759-1766.
65. R. G. Pearson, *J. Am. Chem. Soc.*, 1963, **85**, 3533-&.
66. R. G. Pearson, *J. Chem. Educ.*, 1968, **45**, 581-&.
67. R. G. Pearson, *J. Chem. Educ.*, 1968, **45**, 643-648.
68. R. G. Pearson, *Chemical Hardness*, Wiley-VCH, Weinheim, Germany ; New York, 1997.
69. A. V. Nizovtsev, A. Scheurer, B. Kosog, F. W. Heinemann and K. Meyer, 2013, **2013**, 2538-2548.
70. F. Michel, S. Hamman, C. Philouze, C. P. Del Valle, E. Saint-Aman and F. Thomas, *Dalton Trans.*, 2009, 832-842.
71. G. W. Gokel, R. P. Widera and W. P. Weber, *Org. Synth.*, 1976, **55**, 96.
72. Y. Shi, C. Hall, J. T. Ciszewski, C. Cao and A. L. Odom, *Chem. Commun.*, 2003, 586-587.
73. J. Okuda, S. Fokken, H. C. Kang and W. Massa, *Chem. Ber.*, 1995, **128**, 221-227.
74. B. S. Billow, T. J. McDaniel and A. L. Odom, *Nature Chem.*, 2017, **9**, 837.

